COMPUTERS AND BIOMEDICAL RESEARCH 19, 520–534 (1986)

Spectral and Cross-Spectral Analysis of Heart Rate and Arterial Blood Pressure Variability Signals

G. BASELLI,*† S. CERUTTI,* S. CIVARDI,* D. LIBERATI,* F. LOMBARDI,‡ A. MALLIANI,‡ AND M. PAGANI‡

*CNR Centro Teoria dei Sistemi, Dipartimento di Elettronica, Politecnico di Milano, Milan; †Dipartimento di Automazione Industriale, Università di Brescia, Brescia; and ‡Patologia Medica, "Centro Fidia," Ospedale L. Sacco, Università di Milano, Milan, Italy

Received December 31, 1985

A parametric method for autoregressive (AR) auto- and cross-spectral analysis is presented for the contemporaneous processing of heart rate and arterial blood pressure variability signals. In particular, the introduced bivariate spectral analysis (phase and coherence spectra) provides quantitative and objective means which are useful to measure the role played by the neural controlling systems (sympathetic and parasympathetic systems) on the cardiovascular signals under different pathophysiological conditions. Algorithmic aspects, connected to the way of processing discrete numerical series synchronized to single cardiac beats, are particularly stressed. Important applications are foreseen both in physiological studies and in clinical practice as an aid to the detection of various relevant cardiovascular pathologies such as hypertension and diabetes.

INTRODUCTION

Since the time of the earliest measurements of arterial blood pressure (ABP) and of the electrical activity of the heart (ECG) it was noticed that signals of cardiovascular origin, though almost periodical, were characterized by slight cycle-by-cycle variations (oscillations) in both amplitude and time duration. Discrete series describing these oscillations (either as a function of cardiac cycles or, equivalently, as time functions obtained from these variables by means of interpolation techniques) are generally referred to as variability signals. However, since the development of ABP recording techniques it was noticed that wave amplitude variations had different cyclical patterns not only synchronous with breathing activity but also with longer periods of about 10–20 beat duration, which are frequently referred to as Mayer waves (*1, 2, 3, 4, 5*). These short duration rhythms are normally present and superimposed to slower ones (consisting in very long period oscillations, e.g., circadian rhythm).

The time windows usually considered in studying the mentioned fast variability phenomena are usually in the order of few minutes or hundreds of beats; in addition most of the techniques described below are well suited for the descrip-

0010-4809/86 $3.00

tion of records free of transient phenomena (e.g., change of posture, patient's movements, dynamic physical stress test, etc.) being best candidate to be described as stationary. On the other hand, an accurate quantitative measure of the discrete variability series, with the relevant post processing procedures both in time (autocorrelation function) and in frequency domains (Fourier analysis and power spectral estimation) could become available only with the introduction of proper algorithms for a fast and accurate calculation of the discrete Fourier transform (the fast Fourier transform or FFT) (*6*). The FFT algorithm allowed to perform in a very fast and reliable way various digital operations on signals such as filtering, convolution, and nonparametric calculation of the power spectrum (*7*).

Since the late 60's spectral analysis techniques based on the FFT algorithm have been extensively applied to quantitatively describe the periodical oscillations in variability signals; in particular, the heart rate variability (HRV), based on successive *R-R* duration measurements, has been extensively investigated as it can be obtained from noninvasive ECG recordings, by means of very simple computations (*8, 9*).

Parametric identification techniques (*10*), in particular the autoregressive (AR) ones, appear to be well suited for the description of the HRV signal, as the above-mentioned fluctuations (though cyclical) seem to be properly modeled by a stochastic system. The relevant power spectral density (PSD) estimate is strictly related to maximum entropy spectral estimate (MESE) theory (*11*): the application of these techniques to HRV signal has proved to satisfy the identification hypotheses for reasonable model orders and to lead to statistically more consistent, smoother, and better readable PSD estimates (*12, 13, 14*). A further advantage is in the applicability of spectral decomposition techniques (*15*) which permits us to separately quantify the contributions to overall variability due to the different phenomena clearly visible in the spectra under the form of more or less sharp peaks (*16, 17*).

The PSD analysis of HRV signal seems capable of contributing to the functional investigation into various pathophysiological states (e.g., hypertension, diabetes, ischemic heart disease, etc.) (*18, 19*) or during patient treatment with drugs (*20*). Furthermore, recent studies carried out on both animals and humans, clearly indicate the potential importance of this type of analysis for a quantitative evaluation of the role of the autonomic nervous system in the genesis of these rhythms as clearly visible in the spectra (power and frequency of variability components). Particularly, the rhythm with a period of nearly 10 sec, henceforth called the 10-sec rhythm seems to be a marker of the interaction between the sympathetic and parasympathetic systems (*18, 20, 21, 22, 23, 24*).

In the comprehension of the mechanisms involved in the regulation of the cardiovascular function, the simultaneous observation of ABP and HR variability spectra reveals (under normal conditions) the presence of the 10-sec rhythm (as well as the respiratory rhythm) in both the signals (*25, 26, 27*). Furthermore, animal experiments have indicated that they vary in power under particular

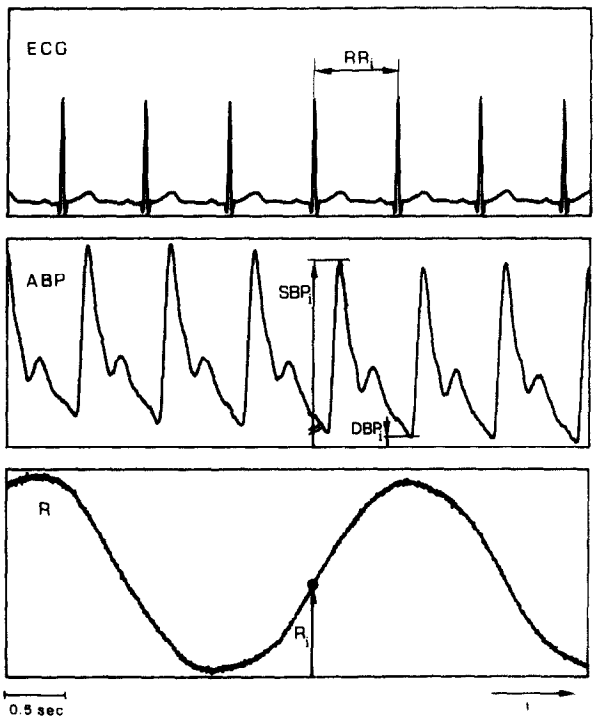

FIG. 1. ECG, arterial blood pressure (ABP) and respiration (R) contemporaneously recorded as a function of time (t). The relevant cycle-by-cycle parameter extraction is indicated at ith cycle: R-R interval (RR_i), systolic blood pressure (SBP_i), diastolic blood pressure (DBP_i) and respiration (see text).

experimental conditions, such as pharmacological neural blockade or cardiac pacing, etc. (*28*).

The cross-spectral analysis of ABP and HR variability signals and the study of the relevant coherence and phase spectra could importantly contribute in the description of the amount of power interchanged between the signals, of the delays by which the rhythms propagate (*29, 30, 31*), and also of the role of respiration. The application of parametric bivariate analysis methods is assumed to deliver better estimates to accomplish this task.

CARDIOVASCULAR VARIABILITY SIGNALS: EXTRACTION OF PARAMETERS

As shown in Fig. 1 a set of measurements is extracted from ECG, ABP, and respiration signal (R) simultaneously recorded, at each ith cardiac cycle. Cardiac cycle duration is measured as the interval between two consecutive R waves, R-R_i; the ith systolic blood pressure (SBP_i) measurement corresponds to the R wave at the beginning of the interval, thus being included into the interval itself; the diastolic pressure (DBP_i) follows SBP_i [a different convention is adopted in Ref. (*30*)]. The two last discrete series are hence called *systogram* and *diastogram* by analogy with the first one called *interval tachogram* or simply *tachogram*.

The ith pulse pressure is thus the difference between SBP_i and DBP_{i-1}; one respiration value R_i is taken as a reference in correspondence with every QRS complex recognized. More values of respiration signal per cardiac cycle may be considered in order to have a broader band description of the signal itself. In the next section reference is made to the detection criteria of these fiducial points. The adopted conventions, though somewhat arbitrary, have to be kept in mind for the quantitative interpretation of results relevant to phase shifts and lags between the different variability signals.

These discrete series, functions of the heart beat index i, are directly processed with an approach similar to the one described in (*30*), avoiding the time interpolation carried on with various techniques introduced by others (*21, 28*). As a matter of fact, it is impossible to make an a priori decision of which one of these two alternative approaches better suits the studying of the interactions between HR and ABP: the heart contraction acts once per cardiac cycle on the vascular systems and arterial pressure peak value is sensed once per beat by arterial baroceptors; on the contrary, neural latencies are preferably measured in seconds, like the delays in the contraction of arterial smooth muscles or the duration of breathing cycles. Fortunately, R-R variability in normal sinus rhythm is of the order of 10% of the mean $\overline{R\text{-}R}$ value, therefore errors introduced in computing time durations by multiplying beat counts by $\overline{R\text{-}R}$ is limited. For the same reason, spectral analysis having frequencies measured in cycles/beat (c/b) is comparable with good approximation to that obtained by the latter, with frequencies in Hertz, as extensively shown in (*32*). Frequency units with [Hz] dimension obtained multiplying [c/b] by [$1/(\overline{R\text{-}R})$] have been referred to as equivalent Hz (eq. Hz) to point out the approximation involved.

Processing Methods Related to Variability Signals

The vector of measurements taken at the ith cardiac cycle will be represented as $x(i) = \text{col}|x_1(i)x_2(i) \ldots x_L(i)|$ where L is the number of different measurements. The series $\{x(i)\}$ with $i = 1, 2, \ldots N$ is described as a finite set of a realization of a stationary discrete-time multivariate process. For simplicity of notation $\{x(i)\}$ is characterized by zero mean, i.e., the mean values have been computed and subtracted from the original measurements (and also stored as indicative parameters of the examined data).

The second order properties of the process is described by the $(L \times L)$ matrix correlation function (MCF)

$$R(k) = E[x(i)x(i-k)^{\mathrm{T}}] \qquad k = 0, \pm 1, \pm 2, \ldots,$$

where the superscript T indicates transposition and k is the lag number. The diagonal element of $R(\cdot)$ is the monovariate autocorrelation functions (ACF) $r_n(\cdot)$ of the nth signal, while element (n, m) is the cross-correlation function (CCF) of series n and m (m and $n = 1, 2, \ldots L$).

The matrix spectral distribution $S(f)$ is the z transform of $R(\cdot)$ evaluated in $z = e^{2j\pi f}$ where f is the normalized frequency: [cycles/sample] or [c/b] in the

present case. Power spectral density distributions (PSD) are on the diagonal, while cross spectra (CS) are the other elements.

If $p + 1$ lags of the MCF are known $R(0) \ldots R(p)$, the maximum entropy method (MEM) defines an infinite extrapolation of the MCF (maximizing the process entropy), which is the MCF of the autoregressive (AR) process of order p computed through the Yule–Walker equations (YW) (*33*). The problem has been first studied and extensively described for the scalar case (*11, 34, 35*).

In the multivariate problem both forward and backward AR models have to be considered in the YW equations, being not equivalent as in the scalar case.

The forward model is defined by the equation

$$\sum_{0}^{p} {}_{k}A_{k}x(i-k) = e_{f}(i)$$

where A_k is the coefficient matrix ($A_0 = I$, identity matrix) and $e_f(\cdot)$ is a white process with variance matrix P_f.

It is worth noting that in this way a canonical form has been arbitrarily imposed on the multivariate process, but as our major concern is the spectral analysis, the problem of univocal spectral factorization is not considered as in the approaches introduced in recent literature which deal with both theoretical (*33, 36*) and applicative aspects (*37*). On the other hand, attention should be devoted to the question mentioned above when one aims at system parametric identification, as pointed out in (*38, 39*).

Defining the polynomial matrix

$$A(z) = \sum_{0}^{p} {}_{k}A_{k}z^{-k}$$

the process may be viewed as the output of a linear, time-invariant system with transfer matrix $A^{-1}(z)$ fed by the white process $e_f(\cdot)$.

Analogously for the backward model, the transfer matrix $B^{-1}(z)$ is defined by

$$B(z) = \sum_{0}^{p} B_{p-k}z^{-k} \qquad (B_0 = I)$$

which is related to the linear block fed by the backward linear prediction process $e_b(\cdot)$, which is white and with variance matrix P_b.

The MESE is thus obtained (*33*) as follows:

$$S(k) = A^{-1}(z)P_{f}A^{-1}(z^{-1}) = B^{-1}(z)P_{b}B^{-1}(z^{-1}).$$

In practical cases a set of data is given rather than a set of correlation lags, thus an ad hoc adaptation of the MEM is accomplished starting with an estimation of the desired lags (*40*). For that reason it is important to evaluate the optimal model order p in order to decide how many lags have to be used as input to the MEM. The task is performed by minimizing the figures FPE and AIC (*33, 37*) whose multivariate versions are given by

$$\text{FPE} = \left(\frac{N + Lp + 1}{N - Lp - 1}\right)^L \det(P)$$

$$\text{AIC} = N \log[\det(P)] + 2L^2p,$$

where $\det(P)$ is the determinant of the matrix P, which represents the mean value of P_f and P_b estimates.

It is also important to verify the identification hypotheses, by testing the whiteness of the prediction errors e_f and e_b. That is accomplished by means of Anderson and χ^2 tests on the prediction process autocorrelation and cross-correlation lags (*10*).

In the present paper the autospectra are first evaluated separately by means of scalar AR identification accomplished via Levison–Durbin algorithm (*41*) as described in (*13, 14*). By means of the scalar AR model poles, a spectral decomposition method (*15*) is applied in order to evaluate the power and the central frequency of each relevant component (see Fig. 3). As described in (*16, 17*) the rationale of the method is in decomposing the ACF into the sum of damped sinusoids with frequencies equal to the AR pole phases. Bivariate analysis is applied to evaluate the CS $C_{nm}(f)$ of the two series (n and m) at a time. Phase $\Phi_{nm}(f)$ and amplitude $G_{nm}(f)$ cross spectra are plotted together with the squared coherence function

$$k^2_{nm}(f) = \frac{C_{nm}(f)C^*_{nm}(f)}{S_n(f)S_m(f)},$$

where $S(f)$ are the autospectra of the input series.

Different recursive algorithms for the computation of the AR parameters do exist, being basically normalizations of the Levison-Wiggins-Robinson (LWR) algorithm (*42*), designed to obtain equal spectral estimates from forward and backward AR models (*36, 43*). The approach described in (*36*) has been adopted, as it has the desirable property of generating stable models at each iteration, being also supposed to have better frequency resolution. The method is based on the direct evaluation of the reflection coefficients performed at each iteration directly on the data, by evaluating the forward and backward prediction error variance matrixes via the parameters of the model of previous iteration.

Reference is made to (*36*) for a complete description of the model and to (*33*) for exhaustive discussion about its characteristics. The cross spectra and the relevant squared coherence have also been computed through the bivariate analog of Bartlett spectral estimates via FFT computation over data subsets and averaging of the obtained cross spectra as described in (*44*).

The periodogram computation has also been used for the spectral analysis of the series $\{R_i\}$ relevant to respiration: this signal was considered only to give a reference value for determining the breathing frequency and its bandwidth in order to have a better interpretation of the spectral analysis brought on over the other variability series, mainly for the correct singling out of the breathing contribution to the overall variability power.

Experimental Protocol

Acquisition, A/D conversion, and preprocessing procedures are carried out at Patologia Medica, "Centro Fidia" Ospedale L. Sacco, Milan. Precordial ECG (V_2 lead), arterial blood pressure (via a 3F Millar microtip transducer catheter, inserted percutaneously into the brachial artery) (*25*) and respiratory movements (via a thoracic belt) are simultaneously recorded.

The results shown in the present paper are intended to simply illustrate the methodologies and the most relevant features of the proposed processing algorithms and are obtained on a set of about 30 subjects consisting of either normal or hypertensive subjects. Other papers will deal with the statistical significance of the processing procedure in the diagnostic classification on a larger set of cases.

The three signals are simultaneously sampled at 300 Hz sampling rate per signal and 12-bit precision, on a Digital Equipment Corporation PDP 11-24 computer. Standard preprocessing and filtering are carried out directly in the above-mentioned hospital, while software development of the multivariate AR approach and the graphic results are obtained at the Department of Electrical Engineering, Polytechnic in Milan, on a DEC VAX 750 computer.

The three signals (see Fig. 1) are processed simultaneously for variability series extraction: QRS complexes are detected via a classical adaptive derivative/threshold algorithm described in (*13*) and the synchronized measurements relevant to each cardiac cycle are stored in the computer memory as well as on a digital tape. The relevant variability signals are hence obtained and shown in Fig. 2.

In this paper examples of spectral and cross-spectral analysis will be shown in a normotensive subject, both at rest and during a passive orthostatic stimulus, i.e., tilt. This is obtained by electrically rotating a motor driven table, where the patient is lying comfortably. This maneuver usually results in a reflex activation of sympathetic activity to the cardiovascular system. A sample of 512 consecutive cardiac cycles is considered for the analysis before tilting and after the transient phenomenon induced on cardiovascular system is elapsed. A similar analysis is performed in a hypertensive subject during daytime and night time (*24*).

Experimental Results

Figure 3 displays the AR PSD and the relevant spectral decomposition of tachogram (a), systogram (b), and diastogram (c) of a normal subject in clinostatic position; the averaged periodogram of respiration is also displayed (d). In (a–c) the central frequency (in eq. Hz), total and percentage power of each component are also displayed. Power units are in [sec^2] for tachograms, [mm Hg^2] for ABP series, and arbitrary units for respiration. Two main components are detectable into the three variability signals: one at approximately 0.1 eq. Hz corresponding to the so-called 10-sec rhythm (Mayer waves), the other coinciding with respiration, being centered on the respiration periodogram peak. The

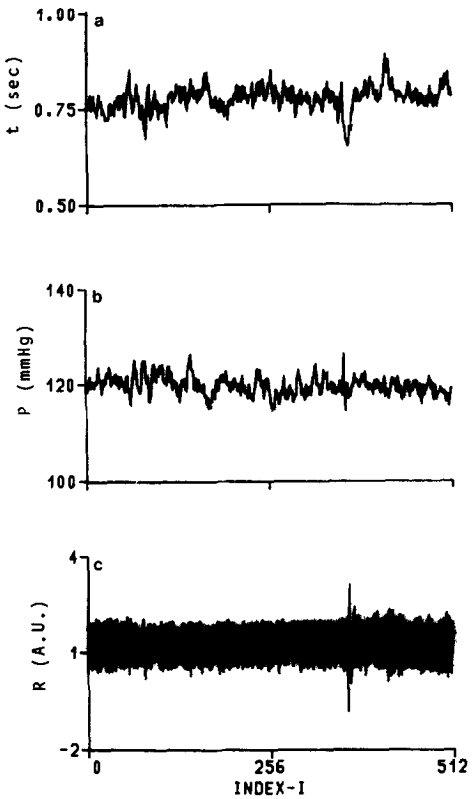

FIG. 2. Variability signals from raw signals in Fig. 1: tachogram (a), systogram (b), and respirogram (c), as a function of index I (no. of cardiac beats).

decomposition algorithm estimates a slightly higher central frequency (0.13 eq. Hz) for the 10-sec rhythm in the tachogram than in the systogram and the diastogram (0.11 eq. Hz).

The respiratory component is centered around 0.33 eq. Hz in both the tachogram and the systogram. This frequency corresponds to the power peak in respiration; in this case the same component is almost absent in the diastogram: some residual power is left around 0.25 Hz; that is due to a cancellation effect related to the null phase shift between tachogram and systogram at 0.33 eq. Hz, as reported in (*30*). The large components displayed at very low frequencies are due to slow trends and rhythms not resolved in the present analysis of 512 beats.

The tachogram-systogram and tachogram-diastogram cross-spectral analysis via bivariate MEM are represented in Figs. 4 and 5, respectively, displaying the cross spectra (a), phase (b, light line), and squared coherence (b, heavy line). This analysis indicates that the 10-sec and the respiratory rhythms are simultaneously and coherently present in both *R-R* interval series and ABP variability. The presence of the two rhythms is particularly evident in the tachogram-

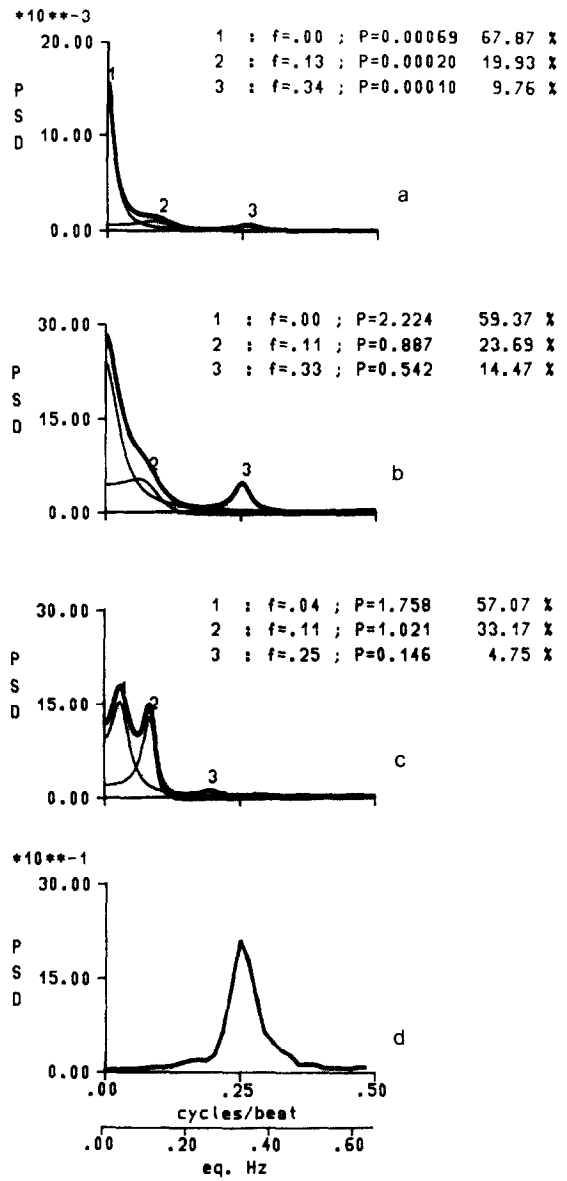

FIG. 3. Normal subject in resting condition. Power spectral density (PSD) of tachogram (a), systogram (b), diastogram (c), and respiration (d). (a), (b), and (c) are estimated via AR modeling and (d) via the periodogram computation. The horizontal axis has a double scale (*c/b* and eq. Hz, see text). The spectral components are also shown for (a), (b), and (c) with their central frequency (in eq. Hz) and power in absolute and percentage value.

systogram amplitude cross spectrum (Fig. 4a). Coherence is also high in the two bands, thus indicating that the power of the two rhythms is well above uncorrelated noise (Fig. 4b). Less amplitude and coherence is displayed in

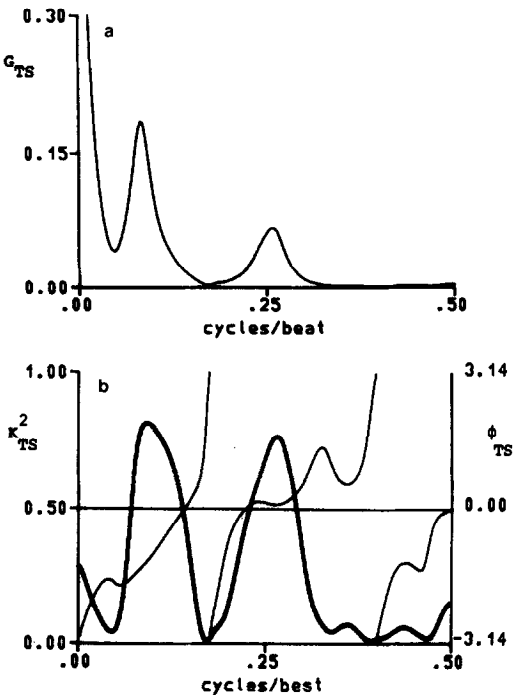

FIG. 4. Normal subject in resting condition (same data as in Fig. 3). AR bivariate analysis of tachogram and systogram: amplitude cross spectrum (a), phase spectrum (b, light line), squared coherence (b, heavy line).

tachogram-diastogram cross-spectrum at respiratory frequency, in relation to the diminished power in the diastogram respiratory component.

When plotting these diagrams, the convention has been adopted that the tachogram leads for positive values while ABP variability leads for negative ones.

Considering Fig. 4b it may be noted that systogram leads at a phase angle of about 60° (i.e., about 2 beats over a 12-beat period) in the 10-sec rhythm, while a null phase shift is found at respiratory frequency: on the other hand positive trend is present almost at all frequencies.

A $\pm \pi$ phase shift between tachogram and diastogram is displayed in Fig. 5b, due to the runoff effect (i.e., the longer the cardiac cycle, the greater the diastolic pressure decay). As an example of spectral analysis carried on via FFT calculation of the periodogram, the tachogram-systogram phase and squared coherence spectra of the same data are displayed in Fig. 6; both diagrams are directly comparable with those shown in Fig. 4b.

Other results are in good accordance with those obtained via FFT techniques by de Boer (*30, 31*).

The same normal subject was studied in a sympathetic activation induced by tilt. The considered epoch of 512 samples starts 5 min after the change of posture to ensure that the effect of transients have disappeared.

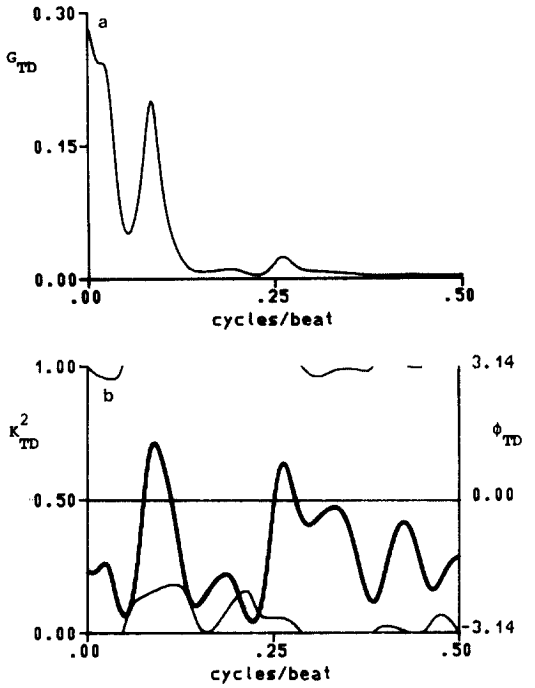

FIG. 5. Normal subject in resting condition (same data as in Fig. 3). AR bivariate analysis of tachogram and diastogram: amplitude cross spectrum (a), phase spectrum (b, light line), squared coherence (b, heavy line).

In this condition a twofold decrease in respiratory component and a slight increase in the 10-sec rhythm was noticed in all the variability signals in accordance to (*18, 20, 25*). This effect is likely to be the consequence of a different interaction between sympathetic and vagal activities.

As shown in Fig. 7, coherence between tachogram and systogram is still high not only in the 10-sec band but also in the respiratory one. No relevant change in the phase diagrams are noticed.

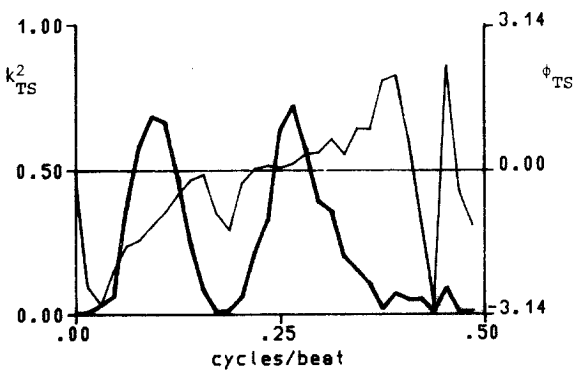

FIG. 6. Same bivariate analysis as in Fig. 4b performed via smoothed periodogram.

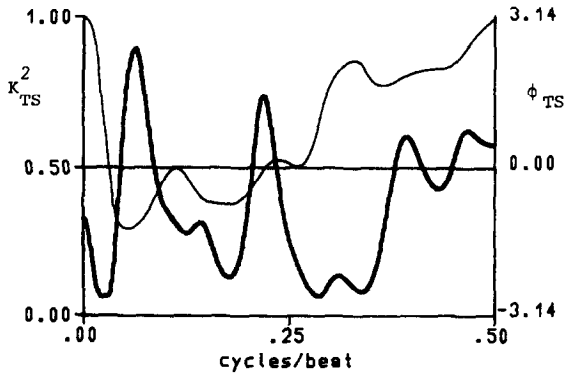

FIG. 7. Normal subject in orthostatic position. AR bivariate analysis of tachogram and systogram: phase spectrum (light line) and squared coherence (heavy line).

It is worth mentioning that a reduced respiratory component is present in the hypertensive subject during daytime (Fig. 8a). In this case there is absence of coherence at the respiratory frequency. In the same hypertensive subject at night time, the power of the respiratory component in both the tachogram and the systogram is similar to that of the low frequency component. This is accompanied by a high coherence (Fig. 8b). In both epochs the coherence at the 10-

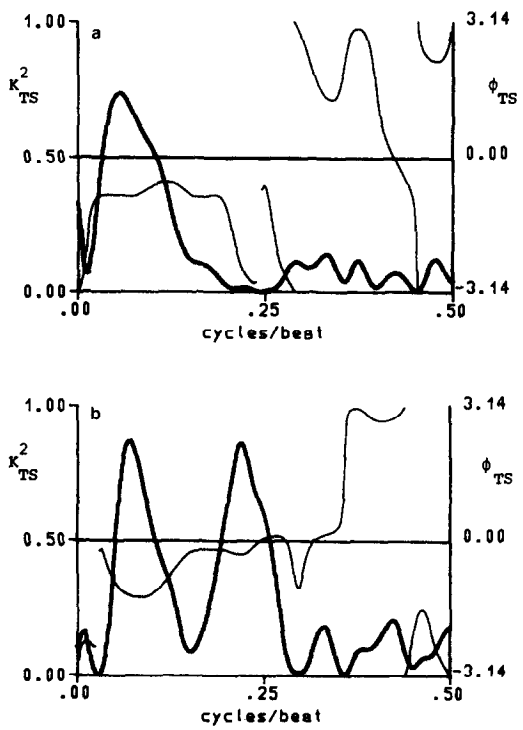

FIG. 8. Hypertensive subject at day time (a) and at night time (b). AR bivariate analysis of tachogram and systogram: phase spectra (light lines) and squared coherence spectra (heavy lines).

sec rhythm is high and the phase shift at this frequency is similar to that observed in the normotensive subject. The phase shift in the respiratory band is null at night time while it is not measurable during day time as coherence is low.

CONCLUSION

Heart rate and blood pressure variability signals can provide important information on the pathophysiology of the cardiovascular regulatory mechanisms, mainly effected by the autonomic nervous system with its sympathetic and parasympathetic components. Spectral and cross-spectral analysis of these variability signals gives quantitative information which can be of potential interest to both physiological and clinical studies. Innovative methodologies based upon bivariate autoregressive (AR) identification and parametric power spectral density estimation introduce autospectra, phase spectra and coherence which completely characterize the physiological relations between the two signals in terms of exchanging powers and statistically consistent phase relationships in determined frequency bands. The two basic rhythms (one around 0.1 Hz and the other around the respiratory frequency), their powers and phases appear capable of describing the changes induced in cardiovascular controls by physiological stimuli such as tilt and disease states such as hypertension.

AR parametrization allows us to obtain maximum entropy spectra and to decompose them in single spectral components in an automatic way: that is an enormous advantage in respect to the traditional techniques based upon nonparametric methods. Further investigations should use extensively the proposed techniques to evaluate their importance in clinical studies.

ACKNOWLEDGMENTS

The present paper has been partially supported by a grant from the Italian Ministry of Education—Special Project on Cardiovascular System—and by a Fellowship of Tecnobiomedica s.p.a., Pomezia, Rome.

REFERENCES

1. TRAUBE, L. Über periodische Tätigkeitsänderungen des vasomotorischen und Hemmungs-Nervenzentrum. *Cbl. Med. Wiss.* **56,** 880 (1865).
2. HERING, E. Uber den Einfluss der Atmung auf den Kreislauf. *Sber. Akad. Wiss. Wien* **60,** 829 (1869).
3. CION, E. Zur Physiologie des Gefässnervenzentrums. *Pflügers Arch.* **9,** 499–513 (1874).
4. MAYER, S. Uber spontane Blutdruckschwankungen. *Sber. Akad. Wiss. Wien.* **74,** 281 (1876).
5. PENAZ, J. Mayer waves: History and methodology. *Automedica (NY)* **2,** 135–141 (1978).
6. COOLEY, J. W., AND TUKEY, J. W. An algorithm for the machine calculation of complex Fourier series. *Math. Comput.* **19,** 297–301 (1965).
7. OPPENHEIM, A. V., AND SHAFER, R. W. "Digital Signal Processing." Prentice-Hall, New York, 1975.
8. SAYER, B. MCA. Analysis of heart rate variability. *Ergonomics* **16,** 85–97 (1973).

9. HYNDMAN, B. W., KITNEY, R. I., AND SAYERS, B. MCA. Spontaneous rhythms in physiological control systems. *Nature (London)* **233,** 339–341 (1974).
10. BOX, G. E. P., AND JENKINS, G. M. "Time Series Analysis: Forecasting and Control." Holden-Day, San Francisco, 1976.
11. BURG, J. P. "Maximum Entropy Spectral Analysis," Proc. 38th Annu. Int. Meeting Soc. of Explor. Geophys. Oklahoma City, 1967.
12. BARTOLI, F., BASELLI, G., AND CERUTTI, S. Application of Identification and Linear Filtering Algorithms to the R-R Interval Measurement. *In* "Proc. IEEE Comput. in Cardiol. Conf., Seattle," 1982.
13. BARTOLI, F., BASELLI, G., AND CERUTTI, S. AR identification and spectral estimate applied to the R-R interval measurements. *Int. J. Bio-Med. Comput.* **16,** 201–215 (1985).
14. BASELLI, G., AND CERUTTI, S. Identification techniques applied to processing of signals from cardiovascular systems. *Med. Inf.* **10,** 223–235 (1985).
15. ZETTERBERG, L. H. Estimation of parameters for a linear difference equation with application to EEG analysis. *Math. Biosci.* **5,** 227–275 (1979).
16. CERUTTI, S., BASELLI, G., AND LIBERATI, D. Autoregressive filtering in heart rate variability signal. *In* "Digital Signal Processing-84." (V. Cappellini and A. G. Costantinides eds.). North Holland, 1984.
17. CERUTTI, S., BASELLI, G., CIVARDI, S., LOMBARDI, F., MALLIANI, A., AND PAGANI, M. Parametric identification and power spectral estimation in heart rate variability signal. *In* "Proc. ISAM Symposium, Padua," 1985.
18. PAGANI, M. *et al.* Power spectral density of heart rate variability as an index of sympatho-vagal interaction in normal and hypertensive subjects. *J. Hypertens.* **2,** 383–385 (1984).
19. LOMBARDI, F. *et al.* Heart rate variability in the first year after myocardial infarction. *In* "Proc. Diagnosis of myocardial ischemia in man, Pisa," 1985.
20. POMERANZ, B. *et al.* Assessment of autonomic function in humans by heart rate spectral analysis. *Amer. J. Physiol.* **248,** H151–H153 (1985).
21. KITNEY, R. I., AND ROMPELMAN, O. "The Study of Heart Rate Variability." Clarendon, Oxford, 1980.
22. AKSELROD, S., GORDON, D., UBEL, F. A., SHANNON, D. C., BARGER, A. C., AND COHEN, R. J. Power spectrum analysis of heart rate fluctuations: A quantitative probe of beat-to-beat cardiovascular control. *Science* **213,** 220–222 (1981).
23. BROVELLI, M. *et al.* Computerized analysis for an experimental validation of neurophysiological models of heart rate control. *In* "Proc. IEEE Comput. in Cardiol. Conf., Aachen," 1983.
24. PAGANI, M. *et al.*, Power spectral analysis of heart rate and arterial pressure variabilities as a marker of sympatho-vagal interaction in man and conscious dog. *Circ. Res.*, in press (1986).
25. PAGANI, M. *et al.* Continuous recording of direct high fidelity arterial pressure and ECG in ambulatory patients. *Cardiovasc. Res.*, in press (1986).
26. ROMPELMAN, O., AND KITNEY, R. I. "The Analysis of Heart Rate Variability and Blood Pressure Fluctuation," Int. Workshop, Delft, 1982.
27. KITNEY, R. I., FULTON, T., MCDONALD, A. H., AND LINKENS, D. A. Transient interactions between blood pressure, respiration and heart rate in man. *J. Biomed. Eng.* **7,** 217–224 (1985).
28. AKSELROD, S., GORDON, D., MAWED, J. B., SNIDMAN, N. C., SHANNON, D. C., AND COHEN, R. J. Beat-to-beat variability in hemodynamic parameters. *Amer. J. Physiol.* in press (1986).
29. ZWIENER, U. Physiological interpretation of autospectra, coherence and phase spectra of blood pressure, heart rate, and respiration waves in man. *Automedica (NY)* **2,** 161–169, 1978.
30. DE BOER, R. W., KAREMAKER, J. N., AND STRACKEE, J. Relationships between short-term blood-pressure fluctuations and heart-rate variability in resting subjects. *Med. Biol. Eng. Comput.* **23,** 352–364 (1985).
31. DE BOER, R. W., "Beat-to-Beat Blood-Pressure Fluctuations and Heart-Rate Variability in Man: Physiological Relationships, Analysis Techniques and a Simple Model." Doctoral thesis, Dept. Physiology, University of Amsterdam, 1985.
32. DE BOER, R. W., KAREMAKER, J. M., AND STRACKEE, J. Comparing spectra of a series of point events particularly for heart rate variability data. *IEEE Trans. Biomed. Eng.* **BME-31** 384–387 (1984).

33. HAYKIN, S., AND KESLER, S. Prediction error filtering and maximum-entropy spectral estimation. *In* "Topics in Applied Physics" (S. Haykin Ed.), Vol. 34, pp. 9–70. New York, 1979.
34. VAN DEN BOS, A. Alternative interpretation of maximum entropy spectral analysis. *IEEE Trans. Inf. Theory* **IT-17,** 439–494 (1971).
35. ULRYCH, T. J., AND BISHOP, T. N. Maximum entropy spectral analysis and autoregressive decomposition. *Rev. Geophys. Space Phys.* **13,** 183–200 (1975).
36. MORF, M., VIEIRA, A., LEE, D. T. L., AND KAILATH, T. Recursive multichannel maximum entropy spectral estimation. *IEEE Trans. Geosci. Electron.* **GE-16,** 85–94 (1978).
37. FRANASZCZUK, P. J., BLINOWSKA, K. J., AND KOWALCZYK, M. The application of parametric multichannel spectral estimates in the study of electrical brain activity. *Biol. Cybern.* **51,** 239–247 (1985).
38. AKAIKE, H. Canonical correlation analysis of time series and the use of an information criterion. *In* "System Identification, Advances and Case Studies" (R. K. Mehra and D. Lainiotis eds.). Academic Press, New York, 1976.
39. BITTANTI, S. "Identificazione Parametrica." Clup, Milano, 1981.
40. JAYNES, E. T. On the rationale of maximum entropy methods. *Proc. IEEE* **70,** 939–952 (1982).
41. KAY, S. M., AND MARPLE, S. L. Spectrum analysis: A modern perspective. *Proc. IEEE* **69,** 1380–1418 (1981).
42. WIGGINS, R. A., AND ROBINSON, E. A. Recursive solution to the multi-channel filtering problem. *J. Geophys. Res.* **70,** 1885–1891 (1965).
43. STRAND, O. N. Multichannel maximum entropy spectral analysis. *IEEE Trans. Autom. Control* **AC-22,** 634–640 (1977).
44. CERUTTI, S. *et al.* Methodological aspects for studying the relations between heart rate and blood pressure variability signals. *In* "Proc. Int. Symp. Neural Mech. and Cardiovasc. Disease." S. Margherita Ligure, May, 1985.